SCIEPublish

Article

Adaptive Event-Triggered Control for Multi-Quadrotor Systems under Aperiodically Intermittent Communications

Wenyu Qin, Yizhi Liu, Yueyong Lv * and Guangfu Ma

Department of Control Science and Engineering, Harbin Institute of Technology, Harbin 150001, China; qinwy_hit@163.com (W.Q.); l1z_email@163.com (Y.L.); magf@hit.edu.cn (G.M.)

* Corresponding author. E-mail: lvyy@hit.edu.cn (Y.L.)

Received: 5 November 2024; Accepted: 12 February 2025; Available online: 19 February 2025

ABSTRACT: A novel adaptive event-triggered control strategy is proposed for multi-quadrotor systems under intermittent communications, addressing the leader-follower consensus-seeking problem where the leader has an unknown bounded input. Firstly, an activation time ratio condition is proposed, eliminating the reliance on the maximum time interval of intermittent communication. Secondly, a compensation term related to the leader's unknown bounded input is designed in the controller to compensate for the error caused by intermittent communication in each period. Meanwhile, a prediction method is developed to eliminate the dependence on continuous information of neighboring quadrotors. Zeno behavior is strictly excluded, and communication among quadrotors is efficiently reduced with the designed event-triggering condition. Finally, numerical simulations verify the effectiveness and superiority of the proposed control strategy.

Keywords: Adaptive control; Event-triggered control; Aperiodically intermittent communication; Multi-quadrotor systems

1. Introduction

In recent years, the cooperative control of multi-quadrotor systems (MQSs) has attracted widespread interest owing to its broad prospects [1–4]. Compared to the limitations of a single quadrotor in terms of sensing range, payload capacity, and operational endurance, MQSs demonstrate enhanced robustness and scalability by utilizing swarm intelligence and distributed sensor fusion. Through coordinated task allocation and formation control, these systems can collaboratively complete mission-critical tasks that are difficult or impossible for a single quadrotor to accomplish, such as large area search and rescue operations requiring rapid coverage of complex terrains, coordinated security patrols with real-time threat triangulation capabilities, and distributed environmental monitoring through spatial sampling. The fundamental issues in multi-quadrotor coordination can be categorized into leaderless consensus [5,6] and leader-follower consensus [7,8]. This paper addresses a more general case: the leader-follower consensus-seeking problem, in which the leader's control input is unknown but bounded.

In the studies mentioned above, it was assumed that communication between quadrotors in MQSs is continuous; however, this assumption is unrealistic in practical scenarios. The communication network in MQSs has limited bandwidth, which can lead to network congestion when the number of quadrotors is large—a fundamental constraint arising from the hidden terminal problem and exponential backoff mechanisms in CSMA/CA protocols, where network throughput typically peaks at 15–25 nodes in 2.4 GHz bands before collapsing due to collision storms. While this issue can be addressed by reducing the sampling frequency or by designing a more efficient communication network, these approaches have inherent limitations. A low sampling frequency may result in system instability, whereas a sparse communication network can compromise the robustness of MQSs. To address this issue, an event-triggered control (ETC) strategy was proposed in [9]. This strategy reduces the communication frequency by altering the conditions under which quadrotors communicate. Quadrotors exchange information with their neighbors only when the designed function is satisfied, thereby reducing the communication burden. To further reduce communication between quadrotors, a dynamic triggering mechanism was proposed in [10], introducing a dynamic variable in the event-triggering condition.

https://doi.org/10.70322/dav.2025.10005

This adjustment increases the upper bound of the measurement error required to satisfy the triggering condition. Similar work was also conducted in [11], where a dynamic event-triggering condition and a self-triggering condition were proposed. These dynamic event-triggering mechanisms constrained the measurement error or consensus error by constructing a state-dependent exponential decay function, which could potentially lead to Zeno behavior when this function becomes sufficiently small. A novel dynamic event-triggering condition was proposed in [12] to further prevent Zeno behavior. In this condition, the measurement error was constrained by both the consensus error and a state-dependent exponential function, effectively preventing Zeno behavior and reducing the number of triggered events.

In the aforementioned studies on the ETC strategy, continuous state information, as well as global information—such as the number of quadrotors and characteristics of the communication topology (e.g., adjacency matrix)—was used in the event-triggering conditions. It should be emphasized that such global information is generally unavailable to individual quadrotors in MQSs; instead, each quadrotor can only access local information from its neighboring quadrotors through limited communication channels. Therefore, these ETC strategies were not fully distributed. The distributed and fully distributed ETC strategies were proposed in [13–15], eliminating the need for continuous and global information. In [13], a fully distributed ETC strategy was developed by introducing adaptive gains in the controller and event-triggering condition to replace gains dependent on global information. The real-time state of neighboring agents was estimated by the prediction method. By utilizing the projection operator approach to improve the adaptive controller and dynamic event-triggering condition, a fully distributed adaptive ETC strategy was proposed in [14], addressing the distributed synchronization of networked systems. Additionally, a fully distributed ETC strategy was developed in [15] to solve the formation problem of MQSs with external disturbances. For the leader-follower consensus problem of multiple spacecraft systems, a fully distributed adaptive observer and distributed control laws were proposed in [16] to solve the attitude-tracking problem with an uncertain leader.

In practical scenarios, MQSs inevitably enter communication-denied environments while performing tasks. Therefore, it is essential to study the consensus problem for MQSs under intermittent communications. In [17], an aperiodically intermittent ETC strategy was proposed for the formation problem under intermittent communication environments, providing quasiperiodicity and average activation time ratio conditions as the fundamental criteria for achieving stability. In [18], an aperiodically intermittent ETC protocol was designed to address the fixed-time consensus problem for nonlinear multi-agent systems. Similarly, in [19], an event-triggered intermittent formation control method was designed for MQSs. By introducing an average method, this approach efficiently saves computation resources and communication bandwidth. A composite event-triggered mechanism was proposed in [20] to govern the activation and deactivation of actuators, addressing the spacecraft attitude control problem with intermittent actuator activation.

To the best of the authors' knowledge, although there are many studies on intermittent control, the time intervals of intermittent communication are generally short, and there is little research concerning MQSs. Moreover, there is no literature addressing adaptive ETC for MQSs under aperiodically intermittent communication environments. Therefore, this issue is worthy of further investigation. The contributions are outlined as follows:

(1) A distributed adaptive ETC strategy is proposed for MQSs with linearized dynamics to address the leader-follower consensus-seeking problem under intermittent communications.
(2) A prediction method is proposed to eliminate the reliance on continuous-time information, thus making the ETC strategy distributed. A compensation term is designed in the controller to address the consensus problem for the leader with unknown control inputs, where the exact form of the leader's input is unknown, but the upper bound on these inputs is available.
(3) An activation time ratio condition is proposed, which, compared to [17,18], eliminates the need for specifying a maximum time interval for intermittent communication.
(4) The Zeno behavior is strictly excluded, and unnecessary communication is effectively reduced under the event-triggering condition.

In summary, the proposed adaptive ETC strategy is of both practical and theoretical significance. Practically, it addresses two critical scenarios: (1) maintaining coordination under aperiodic intermittent communication-denied environments, and (2) preventing channel congestion in normal communication environments where traditional time-driven methods may lead to network overload when the number of quadrotors is large. Theoretically, compared to existing studies [16,17], this work advances three aspects: (1) achieving consensus under general directed graphs with aperiodic intermittent communications, (2) eliminating restrictive maximum control activation period constraints, and (3) strictly excluding Zeno behavior. These innovations offer a novel solution that addresses communication constraints and scalability challenges in practical MQSs.

The rest of this paper is structured as follows. Section 2 gives the preliminaries. The adaptive ETC strategy is designed in Section 3 to address the consensus-seeking problem under intermittent communications. Section 4 provides numerical simulations to verify the effectiveness of the proposed strategy. Finally, the main conclusions are presented in Section 5.

2. Preliminaries

2.1. Algebraic Graph Theory

The communication among quadrotors is described by a directed graph $\mathrm{G}=(\mathrm{V},\mathrm{E},\mathrm{A})$, where $\mathrm{V}=\{1,\cdots,N\}$, $\mathrm{E}\subseteq\mathrm{V}\times\mathrm{V}$ denote the nodes and edges set respectively. The adjacency matrix $A=\left[a_{ij}\right]\in\mathrm{R}^{N\times N}$ denotes the connectivity among agents, where $a_{ij}=1$ if $(j,i)\in\mathrm{E}$, and $a_{ij}=0$ otherwise. The Laplacian matrix L of graph G is defined as $\mathrm{L}=\left[l_{ij}\right]\in\mathrm{R}^{N\times N}$ with $l_{ii}=\sum_{j\in\mathrm{V}}a_{ij}$ and $l_{ij}=-a_{ij},i\neq j$. For the general directed graph that contains a directed spanning tree but is not strongly connected, the Laplacian matrix L can be represented as:

$$\mathrm{L}=\begin{bmatrix}\mathrm{L}_F & \mathrm{L}_{LF}\\ 0 & \mathrm{L}_L\end{bmatrix} \tag{1}$$

where $\mathrm{L}_L\in\mathrm{R}^{N_r\times N_r}$ denotes the strongly connected component, $\mathrm{L}_F\in\mathrm{R}^{N-N_r\times N-N_r}$ represents the non-strongly connected subgraph of followers, and $\mathrm{L}_{LF}\in\mathrm{R}^{N-N_r\times N_r}$ is derived from the structure of the Laplacian matrix, 0 denotes the zero matrix with appropriate dimensions. The following lemmas are presented to support the theory.

Lemma 1 [21]. If the directed graph contains a directed spanning tree, the Laplacian matrix L has a simple zero eigenvalue, and all other eigenvalues have positive real parts. Additionally, there exists a symmetric positive definite matrix S such that $\mathrm{S}\mathrm{L}_F+\mathrm{L}_F^{\mathrm{T}}\mathrm{S}>0$.

2.2. Problem Formulation

Consider a MQSs with linearized dynamics, consisting of one leader and $N-1$ followers. The leader's control input can be accessed by at least one follower. The dynamics of each quadrotor are described as:

$$\begin{aligned}\dot{X}_i(t)&=A_tX_i(t)+B_{t,i}U_{t,i}(t)\\ \dot{\Phi}_i(t)&=A_r\Phi_i(t)+B_{r,i}U_{r.i}(t),i=1,\cdots,N\end{aligned} \tag{2}$$

where $X_i=\left[x_i,y_i,z_i,\mu_i,\upsilon_i,w_i\right]^{\mathrm{T}}$ and $\Phi_i=\left[\phi_i,\theta_i,\psi_i,\dot{\phi}_i,\dot{\theta}_i,\dot{\psi}_i\right]^{\mathrm{T}}$ denote the position and velocity vector, and the angle and angular velocity vector, respectively. The control inputs are $U_{t,i}=\left[\phi_i,\theta_i,f_i\right]^{\mathrm{T}}$ and $U_{r,i}=\left[\tau_{x,i},\tau_{y,i},\tau_{z,i}\right]^{\mathrm{T}}$, where f_i is the thrust force and $\tau_{x,i},\tau_{y,i},\tau_{z,i}$ are the attitude control torques. For simplicity, the control strategy is designed for the position subsystem, while the PID controller is employed for the attitude subsystem. The structure of the ETC strategy is shown in Figure 1. The system matrices $A_t,B_{t,i},A_r,B_{r,i}$ are given as follows:

$$A_t=\begin{bmatrix}0&0&0&1&0&0\\0&0&0&0&1&0\\0&0&0&0&0&1\\0&0&0&0&0&0\\0&0&0&0&0&0\\0&0&0&0&0&0\end{bmatrix},B_{t,i}=\begin{bmatrix}0&0&0\\0&0&0\\0&0&0\\0&-g&0\\g&0&0\\0&0&-1/m_i\end{bmatrix}$$
$$A_r=\begin{bmatrix}0&0&0&1&0&0\\0&0&0&0&1&0\\0&0&0&0&0&1\\0&0&0&0&0&0\\0&0&0&0&0&0\\0&0&0&0&0&0\end{bmatrix},B_{r,i}=\begin{bmatrix}0&0&0\\0&0&0\\0&0&0\\1/J_{x,i}&0&0\\0&1/J_{y,i}&0\\0&0&1/J_{z,i}\end{bmatrix} \tag{3}$$

where m_i represents the mass of each quadrotor, $J_{x,i},J_{y,i},J_{z,i}$ denote the moment of inertia. For simplicity, the dynamics of position subsystem of the quadrotor is represented as $\dot{X}_i(t)=AX_i(t)+BU(t)$. To further proceed, the following assumptions are given.

Assumption 1: The pair (A,B) are stabilizable.

Assumption 2: The directed graph G contains a directed spanning tree.

Assumption 3: The leader's control input is bounded, that is, $\sup_{t\geq 0}\|U(t)\|\leq \bar{u}$, where $\bar{u}$ is a known positive constant.

Assumption 4: At the triggering instant t_k^i, agent *i* can obtain the state $x_j(t_{k'}^j)$ and the consensus error $q_j(t_{k'}^j)$ of neighboring agents.

Remark 1. The assumptions presented are reasonable and align with similar research in multi-agent systems. Assumption 1 is a fundamental prerequisite for controller design in modern control theory. Assumption 2 is consistent with assumptions widely adopted in related literature, such as [13–15], and represents a more general condition compared to the undirected graph constraints in [17,18]. Assumption 3 is in line with the bounded input constraints commonly used in leader-follower consensus problems, as seen in works such as [13–15]. Assumption 4, which requires quadrotors to transmit both state and consensus error at triggering instants, is practically feasible, given that modern communication protocols support multi-parameter transmission in a single exchange. These assumptions strike a balance between theoretical necessity and engineering feasibility, while remaining consistent with existing literature.

Since $N_r=1$, the Laplacian matrix is

$$\mathrm{L}=\begin{bmatrix}\mathrm{L}_F&\mathrm{L}_{LF}\\0&0\end{bmatrix} \tag{4}$$

The consensus error is defined as

$$q_i(t)=\sum_{j\in\mathrm{N}_i}a_{ij}\left(X_i(t)-X_j(t)\right) \tag{5}$$

Therefore, the control objective of the considered MQSs (2) is to design a distributed control strategy that guarantees global asymptotic consensus, *i.e.*, the consensus error of all quadrotors converge to zero. Specifically, the following condition holds.

$$\lim_{t\to\infty}\|q_i(t)\|=0,\ i=1,\cdots,N \tag{6}$$

for any initial states $X_i(0), X_j(0), \forall i, j \in \mathrm{V}$. This condition ensures that the MQSs achieve consensus for all quadrotors regardless of their initial positions and velocities.

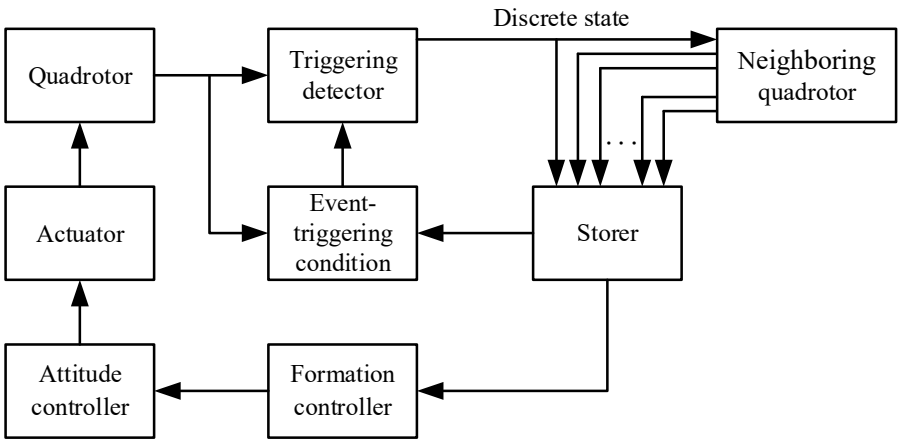

Figure 1. Diagram of the ETC structure under intermittent communications.

A novel ETC strategy is designed in this paper to address the leader-follower consensus-seeking problem under aperiodically intermittent communication environments. As shown in Figure 2, the ETC strategy only operates during the work time intervals, and not during the rest time intervals. The challenge of this paper is to achieve consensus for MQSs within limited work time intervals.

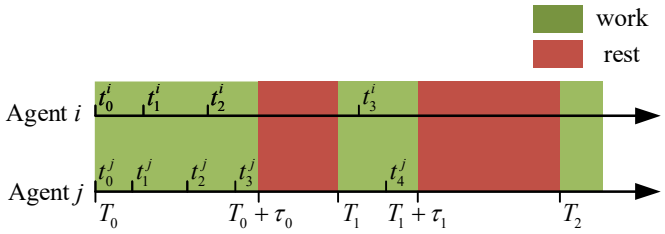

Figure 2. Diagram of event-triggered control under aperiodically intermittent communication environments.

To solve the consensus problem, the following assumption is needed.

Assumption 5: (Activation Time Ratio Condition) There exists a positive constant δ_1 that satisfies $\inf_{i\in\mathrm{N}} \tau_i = \delta_1$ and δ_1 is determined by intermittent communication period and the bound of control input.

Remark 2. The similar activation time ratio condition in [17,18] specifies an upper bound for the control rest period and a lower bound for the control activation period, whereas the activation time ratio condition proposed in this paper only specifies the lower bound. This improvement significantly broadens the applicability of the control strategy, and the selection of δ_1 will be further explained in the following sections.

Remark 3. The leader in MQSs is typically chosen as the root node of the directed graph. This node can send information to its neighbors but cannot receive messages from other agents. The structure of the communication topology is task-dependent and designed to align with specific objectives, such as robustness, scalability, or energy efficiency.

3. Main Results

In this section, a novel ETC strategy is proposed for MQSs under aperiodically intermittent communication environments, effectively addressing the leader-follower consensus-seeking problem where leader has unknown bounded control input. The controller is designed as

$$U(t) = \begin{cases} c_i(t) K q_i\left(t_k^i\right) + (1+\Gamma)\overline{up}\left(K q_i\left(t_k^i\right)\right), t \in \left[T_i, T_i + \tau_i\right) \\ 0 \qquad\qquad\qquad\qquad\qquad\qquad\qquad\quad , t \in \left[T_i + \tau_i, T_{i+1}\right) \end{cases} \tag{7}$$

where $c_i(t)$ and K are adaptive gain and gain matrix, respectively, t_k^i is the k-th triggering instant for agent i, determined by the event-triggering condition to be designed, Γ is defined as

$$\Gamma \geq \frac{\int_{T_{i-1}+\tau_{i-1}}^{T_i} \sum_{i=1}^{N} s_i a_{iN} \left\| Kq_i(s) \right\| ds}{\int_{T_i}^{T_i+\delta_i} \sum_{i=1}^{N-1} s_i a_{iN} \left\| Kq_i(s) \right\| ds} \tag{8}$$

Since the information for the time interval $\left[T_{i-1}+\tau_{i-1}, T_i\right)$ is fully known at the instant T_i, (8) can be derived, $p(\cdot)$ is defined as

$$p(x) = \begin{cases} \dfrac{x}{\|x\|}, & \|x\| \neq 0 \\ 0, & \|x\| = 0 \end{cases} \tag{9}$$

In the proposed controller (7), only the discrete-time states are used, thus avoiding the need for continuous states of neighboring agents and effectively reducing the communication among quadrotors. Since MQSs satisfy Assumption 1, a positive definite matrix P can be obtained by solving the following equation.

$$PA + A^{\mathrm{T}}P - (1-\gamma_1)PBB^{\mathrm{T}}P + \gamma_2 \mathrm{I} = 0 \tag{10}$$

where γ_1 and $\gamma_2 \leq k\lambda_{\max}(P)$ are positive constants, I denotes the identity matrix of appropriate dimensions. The gain matrix is chosen as

$$K = -B^{\mathrm{T}}P \tag{11}$$

The adaptive gain is designed as

$$c_i(t) = \begin{cases} \alpha_i(t) + \beta_i(t), & \text{if } c_i(t) \leq \bar{c} \\ \bar{c}, & \text{if } c_i(t) > \bar{c} \end{cases} \tag{12}$$

where $\alpha_i(t) = \mu_1 k e^{kt} \left\| Kq_i\left(t_k^i\right) \right\|^2$, $\beta_i(t) = \mu_2 \left\| Kq(t) \right\|^2$, $\bar{c}$ is a sufficiently large constant, μ_1 and μ_2 are positive constants. Then, the measurement error is established as

$$e_i(t) = q_i\left(t_k^i\right) - q_i(t) \tag{13}$$

The event-triggering condition is designed as

$$t_{k+1}^i = \left\{ t > t_k^i \,\middle|\, f_1\left(q_i\left(t_k^i\right), q_i(t), t\right) > 0 \vee f_2\left(q_i\left(t_k^i\right), q_i(t), t\right) > 0 \right\} \tag{14}$$

where

$$\begin{aligned} f_1\left(q_i\left(t_k^i\right), q_i(t), t\right) &= \bar{c} \left\| Ke_i(t) \right\| - \vartheta_1 c_i(t) \left\| Kq_i(t) \right\|^2 - \kappa_1 e^{-kt} \\ f_2\left(q_i\left(t_k^i\right), q_i(t), t\right) &= \bar{c}^2 \left\| Ke_i(t) \right\|^2 - \vartheta_2 c_i(t) \left\| Kq_i(t) \right\|^2 - \kappa_2 e^{-kt} \end{aligned} \tag{15}$$

However, the continuous information is still required in (15). To address this issue, the following predicting method is proposed. For the time interval $t \in \left[T_i, T_i + \tau_i\right)$, $q_i(t)$ can be written as

$$\begin{aligned} \dot{q}_i &= \sum_{j \in \mathrm{V}} l_{ij} \left(AX_j + c_j BKq_j\left(t_{k'}^j\right) + (1+\Gamma)\bar{u}Bp\left(Kq_j\left(t_{k'}^j\right)\right) \right) \\ &= Aq_i + l_{ii}c_i BKq_i\left(t_k^i\right) - \sum_{j \in \mathrm{N}_i} a_{ij}c_j BKq_j\left(t_{k'}^j\right) + l_{ii}(1+\Gamma)\bar{u}Bp\left(Kq_i\left(t_k^i\right)\right) - \sum_{j \in \mathrm{N}_i} l_{ij}(1+\Gamma)\bar{u}Bp\left(Kq_j\left(t_{k'}^j\right)\right) \end{aligned} \tag{16}$$

Since all information in (16) is known at the triggering instant t_k^i, $q_i(t)$ can be obtained. By substituting (7) into (2), the MQSs can be described as:

$$\dot{X}_i(t)=\begin{cases}AX_i(t)+c_i(t)BKq_i(t_k^i)+(1+\Gamma)\bar{u}Bp(Kq_i(t_k^i)),t\in[T_i,T_i+\tau_i)\\AX_i(t) \qquad ,t\in[T_i+\tau_i,T_{i+1})\end{cases} \tag{17}$$

Rewrite (17) in a compact form

$$\dot{X}(t)=\begin{cases}(\mathbf{I}\otimes A)X(t)+(\mathrm{C}\otimes BK)(e+q)+(1+\Gamma)(\bar{u}\mathbf{I}\otimes B)P(K,q,e),t\in[T_i,T_i+\tau_i)\\(\mathbf{I}\otimes A)X(t) \qquad ,t\in[T_i+\tau_i,T_{i+1})\end{cases} \tag{18}$$

The consensus error (5) can also be rewrite as

$$q=(\mathrm{L}_F\otimes\mathbf{I})X+(\mathrm{L}_{LF}\otimes\mathbf{I})X_L \tag{19}$$

It is straightforward to obtain that for the time interval $t\in[T_i,T_i+\tau_i)$

$$\dot{q}=(\mathbf{I}\otimes A)q+(\mathrm{L}_F\mathrm{C}\otimes BK)(e+q)+(1+\Gamma)(\bar{u}\mathrm{L}_F\otimes B)H(K,q,e)+(\mathrm{L}_{LF}\otimes B)U_N \tag{20}$$

and for the time interval $t\in[T_i+\tau_i,T_{i+1})$

$$\dot{q}=(\mathbf{I}\otimes A)q+(\mathrm{L}_{LF}\otimes B)U_N \tag{21}$$

The following lemmas are required before presenting the main theorem.

Lemma 2. If a and b are nonnegative constants and p and q are positive constants such that $1/p+1/q=1$, then

$$ab\le\varepsilon\frac{a^p}{p}+\varepsilon^{-1}\frac{b^q}{q} \tag{22}$$

Lemma 3 [21]. Under the event-triggering condition (14), the following inequality holds

$$(a-b)\left\|Kq_i(t_k^i)\right\|^2\le\left(2a-\frac{b\rho}{1+\rho}+\frac{2a\vartheta_2c_i(t)}{\bar{c}^2}+\frac{b\rho\vartheta_2c_i(t)}{\bar{c}^2}\right)\left\|Kq_i(t)\right\|^2+\frac{2a+b\rho}{\bar{c}^2}\kappa_2e^{-\sigma t} \tag{23}$$

for any given constants $t\ge0$, $\rho>0$, $i\in\mathrm{V}$ and constants $a>0$, $b>0$.

Lemma 4 [21]. For $a>0$, $b\ge0$ and $c\ge0$, there exists a sufficiently large constant $d>0$ such that

$$-a\bar{\mathrm{C}}^2+b\mathrm{I}+c\mathrm{S}\bar{\mathrm{C}}-d\mathrm{S}\le-\mathrm{S}\bar{\mathrm{C}} \tag{24}$$

holds for $t\ge0$, where $\bar{\mathrm{C}}=\mathrm{diag}\{\bar{c},\cdots,\bar{c}\}\in\mathrm{R}^{N-1}$.

Lemma 5 [21]. The following inequalities hold

$$q_i^{\mathrm{T}}K^{\mathrm{T}}p(Kq_i+Ke_i)\ge\|Kq_i\|-2\|Ke_i\| \tag{25}$$

$$q_i^{\mathrm{T}}K^{\mathrm{T}}p(Kq_i+Ke_i)\le\|Kq_i\| \tag{26}$$

for $i,j=1,\cdots,N-1$, $i\ne j$.

Then, the main theorem of this paper is given.

Theorem 1. Consider the MQSs (2) satisfy Assumption 1–Assumption 5, the proposed ETC strategy consists of controller (7), adaptive gain (12), and event-triggering condition (14). Then, the leader-follower consensus can be achieved and the Zeno behavior is strictly excluded.

Proof. The proof is organized into four steps. First, the Lyapunov function will be analyzed separately for the intervals $t\in\left[T_i,T_i+\tau_i\right)$ and $t\in\left[T_i+\tau_i,T_{i+1}\right)$. Then, an overall analysis of the Lyapunov function for all time intervals will be conducted. Finally, it will be shown that the proposed control strategy can effectively eliminate Zeno behavior.

Consider a Lyapunov function as

$$V(t)=q^{\mathrm{T}}(t)\left(\mathrm{S}\bar{\mathrm{C}}\otimes P\right)q(t)+\frac{e^{-kt}}{2\mu_1 k}\sum_{i=1}^{N-1}s_i\left(c_i-\bar{c}\right)^2 \tag{27}$$

Take the time derivative of $V(t)$, it yields that

$$\dot{V}(t)=\dot{q}^{\mathrm{T}}(t)\left(\mathrm{S}\bar{\mathrm{C}}\otimes P\right)q(t)+q^{\mathrm{T}}(t)\left(\mathrm{S}\bar{\mathrm{C}}\otimes P\right)\dot{q}(t)-\frac{e^{-kt}}{2\mu_1}\sum_{i=1}^{N-1}s_i\left(c_i-\bar{c}\right)^2+\frac{e^{-kt}}{\mu_1 k}\sum_{i=1}^{N-1}s_i\left(c_i-\bar{c}\right)\dot{c}_i \tag{28}$$

Step 1: For the time interval $t\in\left[T_i,T_i+\tau_i\right)$, substituting adaptive gain $c_i(t)$, gain matrix K yields

$$\begin{aligned}\dot{V}(t)=&q^{\mathrm{T}}\left[\mathrm{S}\bar{\mathrm{C}}\otimes\left(PA+A^{\mathrm{T}}P\right)\right]q-2(1+\Gamma)\bar{u}q^{\mathrm{T}}\left(\bar{\mathrm{C}}\mathrm{SL}_F\otimes K^{\mathrm{T}}\right)P(K,q,e)-2q^{\mathrm{T}}\left(\bar{\mathrm{C}}\mathrm{SL}_F\mathrm{C}\otimes K^{\mathrm{T}}K\right)(e+q)\\&-2q^{\mathrm{T}}\left(\bar{\mathrm{C}}\mathrm{SL}_{LF}\otimes K^{\mathrm{T}}\right)u_N+\sum_{i=1}^{N-1}s_i\left(c_i-\bar{c}\right)\left\|Kq_i\left(t_k^i\right)\right\|^2-\frac{e^{-kt}}{2\mu_1}\sum_{i=1}^{N-1}s_i\left(c_i-\bar{c}\right)^2\end{aligned} \tag{29}$$

It is easy to derive that

$$\begin{aligned}-2q^{\mathrm{T}}\left(\bar{\mathrm{C}}\mathrm{SL}_F\mathrm{C}\otimes K^{\mathrm{T}}K\right)(e+q)=&-2q^{\mathrm{T}}\left(\bar{\mathrm{C}}\mathrm{SL}_F\mathrm{C}\otimes K^{\mathrm{T}}K\right)e-2q^{\mathrm{T}}\left(\bar{\mathrm{C}}\mathrm{SL}_F\bar{\mathrm{C}}\otimes K^{\mathrm{T}}K\right)q\\&+2q^{\mathrm{T}}\left(\bar{\mathrm{C}}\mathrm{SL}_F\bar{\mathrm{C}}\otimes K^{\mathrm{T}}K\right)q-2q^{\mathrm{T}}\left(\bar{\mathrm{C}}\mathrm{SL}_F\mathrm{C}\otimes K^{\mathrm{T}}K\right)q\end{aligned} \tag{30}$$

According to Lemma 1, it yields that

$$\begin{aligned}-2q^{\mathrm{T}}\left(\bar{\mathrm{C}}\mathrm{SL}_F\bar{\mathrm{C}}\otimes K^{\mathrm{T}}K\right)q=&-q^{\mathrm{T}}\left[\bar{\mathrm{C}}\left(\mathrm{SL}_F+\mathrm{L}_F^{\mathrm{T}}\mathrm{S}\right)\bar{\mathrm{C}}\otimes K^{\mathrm{T}}K\right]q\\\le&-\lambda_{\min}\left(\mathrm{SL}_F+\mathrm{L}_F^{\mathrm{T}}\mathrm{S}\right)q^{\mathrm{T}}\left(\bar{\mathrm{C}}^2\otimes K^{\mathrm{T}}K\right)q\end{aligned} \tag{31}$$

According to Lemma 2 and the event-triggering condition (14), the following inequalities can be obtained

$$\begin{aligned}&-2q^{\mathrm{T}}\left(\bar{\mathrm{C}}\mathrm{SL}_F\mathrm{C}\otimes K^{\mathrm{T}}K\right)e\\&\le\xi_1 q^{\mathrm{T}}\left(\bar{\mathrm{C}}\mathrm{SL}_F\mathrm{L}_F^{\mathrm{T}}\mathrm{S}\bar{\mathrm{C}}\otimes K^{\mathrm{T}}K\right)q+\xi_1^{-1}e^{\mathrm{T}}\left(\mathrm{C}^2\otimes K^{\mathrm{T}}K\right)e\\&\le\xi_1\lambda_{\min}\left(\mathrm{SL}_F\mathrm{L}_F^{\mathrm{T}}\mathrm{S}\right)q^{\mathrm{T}}\left(\bar{\mathrm{C}}^2\otimes K^{\mathrm{T}}K\right)q+\xi_1^{-1}\vartheta_2 q^{\mathrm{T}}\left(\mathrm{C}\otimes K^{\mathrm{T}}K\right)q+\xi_1^{-1}N\kappa_2 e^{-kt}\end{aligned} \tag{32}$$

$$\begin{aligned}&2q^{\mathrm{T}}\left(\bar{\mathrm{C}}\mathrm{SL}_F\bar{\mathrm{C}}\otimes K^{\mathrm{T}}K\right)q\\&\le\xi_2 q^{\mathrm{T}}\left(\bar{\mathrm{C}}\mathrm{SL}_F\mathrm{L}_F^{\mathrm{T}}\mathrm{S}\bar{\mathrm{C}}\otimes K^{\mathrm{T}}K\right)q+\xi_2^{-1}q^{\mathrm{T}}\left(\bar{\mathrm{C}}^2\otimes K^{\mathrm{T}}K\right)q\\&\le\xi_2\lambda_{\min}\left(\mathrm{SL}_F\mathrm{L}_F^{\mathrm{T}}\mathrm{S}\right)q^{\mathrm{T}}\left(\bar{\mathrm{C}}^2\otimes K^{\mathrm{T}}K\right)q+\xi_2^{-1}q^{\mathrm{T}}\left(\bar{\mathrm{C}}^2\otimes K^{\mathrm{T}}K\right)q\end{aligned} \tag{33}$$

$$\begin{aligned}&-2q^{\mathrm{T}}\left(\bar{\mathrm{C}}\mathrm{SL}_F\mathrm{C}\otimes K^{\mathrm{T}}K\right)q\\&\le\xi_3 q^{\mathrm{T}}\left(\bar{\mathrm{C}}\mathrm{SL}_F\mathrm{L}_F^{\mathrm{T}}\mathrm{S}\bar{\mathrm{C}}\otimes K^{\mathrm{T}}K\right)q+\xi_3^{-1}q^{\mathrm{T}}\left(\mathrm{C}^2\otimes K^{\mathrm{T}}K\right)q\\&\le\xi_3\lambda_{\min}\left(\mathrm{SL}_F\mathrm{L}_F^{\mathrm{T}}\mathrm{S}\right)q^{\mathrm{T}}\left(\bar{\mathrm{C}}^2\otimes K^{\mathrm{T}}K\right)q+\xi_3^{-1}q^{\mathrm{T}}\left(\bar{\mathrm{C}}^2\otimes K^{\mathrm{T}}K\right)q\end{aligned} \tag{34}$$

Combining (32)–(34), it yields that

$$\begin{aligned}
&-2q^{\mathrm{T}}\left(\overline{\mathrm{C}}\mathrm{SL}_F\mathrm{C}\otimes K^{\mathrm{T}}K\right)(e+q)\\
&\le -\lambda_{\min}\left(\mathrm{SL}_F+\mathrm{L}_F^{\mathrm{T}}\mathrm{S}\right)q^{\mathrm{T}}\left(\overline{\mathrm{C}}^2\otimes K^{\mathrm{T}}K\right)q+\left(\xi_1+\xi_2+\xi_3\right)\lambda_{\min}\left(\mathrm{SL}_F\mathrm{L}_F^{\mathrm{T}}\mathrm{S}\right)q^{\mathrm{T}}\left(\overline{\mathrm{C}}^2\otimes K^{\mathrm{T}}K\right)q\\
&+\left(\xi_1^{-1}\vartheta_2+\xi_2^{-1}\overline{c}+\xi_3^{-1}\overline{c}\right)q^{\mathrm{T}}\left(\overline{\mathrm{C}}\otimes K^{\mathrm{T}}K\right)q+\xi_1^{-1}N\kappa_2e^{-kt}\\
&=-\xi_4q^{\mathrm{T}}\left(\overline{\mathrm{C}}^2\otimes K^{\mathrm{T}}K\right)q+\xi_5q^{\mathrm{T}}\left(\overline{\mathrm{C}}\otimes K^{\mathrm{T}}K\right)q+\xi_1^{-1}N\kappa_2e^{-kt}
\end{aligned}\tag{35}$$

where $\xi_4=\lambda_{\min}\left(\mathrm{SL}_F+\mathrm{L}_F^{\mathrm{T}}\mathrm{S}\right)-\left(\xi_1+\xi_2+\xi_3\right)\lambda_{\max}\left(\mathrm{SL}_F\mathrm{L}_F^{\mathrm{T}}\mathrm{S}\right)$, $\xi_5=\xi_1^{-1}\vartheta_2+\xi_2^{-1}\overline{c}+\xi_3^{-1}\overline{c}$. It is clear that $\xi_4>0$ can be achieved by designing ξ_1, ξ_2 and ξ_3. According to Lemma 5, the following inequality can be derived

$$\begin{aligned}
&-2\left(1+\Gamma\right)\overline{u}q^{\mathrm{T}}\left(\overline{\mathrm{C}}\mathrm{SL}_F\otimes K^{\mathrm{T}}\right)P\left(K,q,e\right)\\
&=2\left(1+\Gamma\right)\overline{cu}\sum_{i=1}^{N-1}\sum_{j=1,j\ne i}^{N-1}s_ia_{i,j}q_i^{\mathrm{T}}K^{\mathrm{T}}p\left(Kq_i\left(t_k^i\right)\right)-2\left(1+\Gamma\right)\overline{cu}\sum_{i=1}^{N-1}s_il_{i,i}q_i^{\mathrm{T}}K^{\mathrm{T}}p\left(Kq_i\left(t_k^i\right)\right)\\
&\le 2\left(1+\Gamma\right)\overline{cu}\sum_{i=1}^{N-1}\sum_{j=1,j\ne i}^{N-1}s_ia_{i,j}\left\|Kq_i\right\|-2\left(1+\Gamma\right)\overline{cu}\sum_{i=1}^{N-1}s_il_{i,i}\left(\left\|Kq_i\right\|-2\left\|Ke_i\right\|\right)\\
&=4\left(1+\Gamma\right)\overline{cu}\sum_{i=1}^{N-1}s_il_{i,i}\left\|Ke_i\right\|-2\left(1+\Gamma\right)\overline{cu}\sum_{i=1}^{N-1}s_ia_{i,N}\left\|Kq_i\right\|\\
&\le 4\left(1+\Gamma\right)\overline{u}\vartheta_1\sum_{i=1}^{N-1}s_il_{i,i}c_i\left\|Kq_i\right\|^2+4\left(1+\Gamma\right)\overline{u}\kappa_1\sum_{i=1}^{N-1}s_il_{i,i}e^{-kt}-2\left(1+\Gamma\right)\overline{cu}\sum_{i=1}^{N-1}s_ia_{i,N}\left\|Kq_i\right\|
\end{aligned}\tag{36}$$

It is easy to obtain from Assumption 3 that

$$\begin{aligned}
&-2q^{\mathrm{T}}\left(\overline{\mathrm{C}}\mathrm{SL}_{LF}\otimes K^{\mathrm{T}}\right)u_N=-2\overline{c}\sum_{i=1}^{N-1}s_ia_{iN}q_i^{\mathrm{T}}K^{\mathrm{T}}u_N\\
&\le 2\overline{c}\sum_{i=1}^{N-1}s_ia_{iN}\left\|Kq_i\right\|\left\|u_N\right\|\le 2\overline{cu}\sum_{i=1}^{N-1}s_ia_{iN}\left\|Kq_i\right\|
\end{aligned}\tag{37}$$

Combining (36) and (37) yields

$$\begin{aligned}
&-2\left(1+\Gamma\right)\overline{u}q^{\mathrm{T}}\left(\overline{\mathrm{C}}\mathrm{SL}_F\otimes K^{\mathrm{T}}\right)P\left(K,q,e\right)-2q^{\mathrm{T}}\left(\overline{\mathrm{C}}\mathrm{SL}_{LF}\otimes K^{\mathrm{T}}\right)u_N\\
&\le 4\left(1+\Gamma\right)\overline{u}\vartheta_1\sum_{i=1}^{N-1}s_il_{i,i}c_i\left\|Kq_i\right\|^2+4\left(1+\Gamma\right)\overline{u}\kappa_1\sum_{i=1}^{N-1}s_il_{i,i}e^{-kt}-2\Gamma\overline{cu}\sum_{i=1}^{N-1}s_ia_{iN}\left\|Kq_i\right\|\\
&\le \xi_6q^{\mathrm{T}}\left(\mathbf{I}\otimes K^{\mathrm{T}}K\right)q+\xi_7e^{-kt}-2\Gamma\overline{cu}\sum_{i=1}^{N-1}s_ia_{iN}\left\|Kq_i\right\|
\end{aligned}\tag{38}$$

where $\xi_6=4\left(1+\Gamma\right)\vartheta_1\overline{uc}\max_{i=1,\cdots,N-1}\left\{s_il_{ii}\right\}$, $\xi_7=4\left(1+\Gamma\right)\overline{u}\kappa_1N\max_{i=1,\cdots,N-1}\left\{s_il_{ii}\right\}$. According to Lemma 3, the following inequality can be obtained

$$\begin{aligned}
\sum_{i=1}^{N-1}s_i\left(c_i-\overline{c}\right)\left\|Kq_i\left(t_k^i\right)\right\|^2&\le\sum_{i=1}^{N-1}s_i\left[\left(2c_i-\frac{\overline{c}\rho}{1+\rho}+\frac{2\vartheta_2c_i^2}{\overline{c}^2}+\frac{\rho\vartheta_2c_i}{\overline{c}}\right)\left\|Kq_i\left(t\right)\right\|^2+\frac{2c_i+\overline{c}\rho}{\overline{c}^2}\kappa_2e^{-kt}\right]\\
&\le q^{\mathrm{T}}\left\{\left[2\mathrm{SC}-\left(\frac{\overline{c}\rho}{1+\rho}-2\vartheta_2-\rho\vartheta_2\right)\mathrm{S}\right]\otimes K^{\mathrm{T}}K\right\}q+\xi_8e^{-kt}
\end{aligned}\tag{39}$$

where $\xi_8=\sum_{i=1}^{N-1}s_i\left(2+\rho\right)\kappa_2/\overline{c}$. Combining (35), (38) and (39) yields

$$\begin{aligned}\dot{V}(t)&\le q^{\mathrm{T}}\left[\mathrm{S}\overline{\mathrm{C}}\otimes\left(PA+A^{\mathrm{T}}P\right)\right]q-\xi_4 q^{\mathrm{T}}\left(\overline{\mathrm{C}}^2\otimes K^{\mathrm{T}}K\right)q+\xi_5 q^{\mathrm{T}}\left(\overline{\mathrm{C}}\otimes K^{\mathrm{T}}K\right)q\\&+\xi_6 q^{\mathrm{T}}\left(\mathbf{I}\otimes K^{\mathrm{T}}K\right)q-2\Gamma\overline{cu}\sum_{i=1}^{N-1}s_i a_{iN}\left\|Kq_i\right\|-\frac{e^{-kt}}{2\mu_1}\sum_{i=1}^{N-1}s_i\left(c_i-\overline{c}\right)^2\\&+q^{\mathrm{T}}\left\{\left[2\mathrm{SC}-\left(\frac{\overline{c}\rho}{1+\rho}-2\vartheta_2-\rho\vartheta_2\right)\mathrm{S}\right]\otimes K^{\mathrm{T}}K\right\}q+\xi_7 e^{-kt}+\xi_1^{-1}N\kappa_2 e^{-kt}+\xi_8 e^{-kt}\\&=q^{\mathrm{T}}\left[\mathrm{S}\overline{\mathrm{C}}\otimes\left(PA+A^{\mathrm{T}}P\right)\right]q-2\Gamma\overline{cu}\sum_{i=1}^{N-1}s_i a_{iN}\left\|Kq_i\right\|-\frac{e^{-kt}}{2\mu_1}\sum_{i=1}^{N-1}s_i\left(c_i-\overline{c}\right)^2+\xi_9 e^{-kt}\\&+q^{\mathrm{T}}\left\{\left[-\xi_4\overline{\mathrm{C}}^2+\xi_6\mathbf{I}+\left(2+\frac{\xi_5}{\lambda_{\min}(\mathrm{S})}\right)\mathrm{S}\overline{\mathrm{C}}-\left(\frac{\overline{c}\rho}{1+\rho}-2\vartheta_2-\rho\vartheta_2\right)\mathrm{S}\right]\otimes K^{\mathrm{T}}K\right\}q\end{aligned}\tag{40}$$

where $\xi_9=\xi_7+\xi_1^{-1}N\kappa_2+\xi_8$. According to Lemma 4, it is easy to obtain that

$$-\xi_4\overline{\mathrm{C}}^2+\xi_6\mathbf{I}+\left(2+\frac{\xi_5}{\lambda_{\min}(\mathrm{S})}\right)\mathrm{S}\overline{\mathrm{C}}-\left(\frac{\overline{c}\rho}{1+\rho}-2\vartheta_2-\rho\vartheta_2\right)\mathrm{S}\le-\mathrm{S}\overline{\mathrm{C}}\tag{41}$$

Substituting (41) into (40) yields

$$\dot{V}(t)\le q^{\mathrm{T}}\left[\mathrm{S}\overline{\mathrm{C}}\otimes\left(PA+A^{\mathrm{T}}P-K^{\mathrm{T}}K\right)\right]q-2\Gamma\overline{cu}\sum_{i=1}^{N-1}s_i a_{iN}\left\|Kq_i\right\|-\frac{e^{-kt}}{2\mu_1}\sum_{i=1}^{N-1}s_i\left(c_i-\overline{c}\right)^2+\xi_9 e^{-kt}\tag{42}$$

According to (10), it is easy to derive that

$$\begin{aligned}\dot{V}(t)&\le-\frac{\gamma_2}{\lambda_{\max}(P)}q^{\mathrm{T}}\left(\mathrm{S}\overline{\mathrm{C}}\otimes P\right)q-2\Gamma\overline{cu}\sum_{i=1}^{N-1}s_i a_{iN}\left\|Kq_i\right\|-\frac{e^{-kt}}{2\mu_1}\sum_{i=1}^{N-1}s_i\left(c_i-\overline{c}\right)^2+\xi_9 e^{-kt}\\&=-\frac{\gamma_2}{\lambda_{\max}(P)}V-2\Gamma\overline{cu}\sum_{i=1}^{N-1}s_i a_{iN}\left\|Kq_i\right\|-\left(1-\frac{\gamma_2}{k\lambda_{\max}(P)}\right)\frac{e^{-kt}}{2\mu_1}\sum_{i=1}^{N-1}s_i\left(c_i-\overline{c}\right)^2+\xi_9 e^{-kt}\end{aligned}\tag{43}$$

Since k and γ_2 are chosen to satisfy $1-\gamma_2/k\lambda_{\max}(P)\ge 0$, the following inequality can be obtained

$$\dot{V}(t)\le-\frac{\gamma_2}{\lambda_{\max}(P)}V-2r\overline{cu}\sum_{i=1}^{N-1}s_i a_{iN}\left\|Kq_i\right\|+\xi_9 e^{-kt}\tag{44}$$

Step 2: For the time interval $t\in\left[T_i+\tau_i,T_{i+1}\right)$, by adopting the same procedures as in the previous section, the following inequality can be derived.

$$\begin{aligned}\dot{V}(t)&\le q^{\mathrm{T}}\left[\mathrm{S}\overline{\mathrm{C}}\otimes\left(PA+A^{\mathrm{T}}P\right)\right]q-2q^{\mathrm{T}}\left(\overline{\mathrm{C}}\mathrm{S}\mathrm{L}_{LF}\otimes K^{\mathrm{T}}\right)u_N+\varepsilon q^{\mathrm{T}}\left(\overline{\mathrm{C}}^2\otimes K^{\mathrm{T}}K\right)q-\frac{e^{-kt}}{2\mu_1}\sum_{i=1}^{N-1}s_i\left(c_i-\overline{c}\right)^2\\&+q^{\mathrm{T}}\left\{\left[-\varepsilon\overline{\mathrm{C}}^2+2\mathrm{S}\overline{\mathrm{C}}-\left(\frac{\overline{c}\rho}{1+\rho}-2\vartheta_2-\rho\vartheta_2\right)\mathrm{S}\right]\otimes K^{\mathrm{T}}K\right\}q+\xi_{10}e^{-kt}\\&\le q^{\mathrm{T}}\left[\mathrm{S}\overline{\mathrm{C}}\otimes\left(PA+A^{\mathrm{T}}P-\left(1-\gamma_1\right)K^{\mathrm{T}}K\right)\right]q-2q^{\mathrm{T}}\left(\overline{\mathrm{C}}\mathrm{S}\mathrm{L}_{LF}\otimes K^{\mathrm{T}}\right)u_N-\frac{e^{-kt}}{2\mu_1}\sum_{i=1}^{N-1}s_i\left(c_i-\overline{c}\right)^2+\xi_{10}e^{-kt}\end{aligned}\tag{45}$$

where ε is a positive constants that satisfies $\varepsilon\le\gamma_1\min\left\{s_1/\overline{c},\cdots,s_{N-1}/\overline{c}\right\}$, substituting (37) into (45) gives

$$\begin{aligned}\dot{V}(t) &\le -\frac{\gamma_2}{\lambda_{\max}(P)} q^{\mathrm{T}}\left(\mathrm{S}\overline{\mathrm{C}}\otimes P\right)q + 2\overline{cu}\sum_{i=1}^{N} s_i a_{iN}\left\|Kq_i\right\| - \frac{e^{-kt}}{2\mu_1}\sum_{i=1}^{N-1} s_i\left(c_i-\overline{c}\right)^2 + \xi_{10}e^{-kt} \\ &= -\frac{\gamma_2}{\lambda_{\max}(P)} V + 2\overline{cu}\sum_{i=1}^{N} s_i a_{iN}\left\|Kq_i\right\| - \left(1-\frac{\gamma_2}{\lambda_{\max}(P)k}\right)\frac{e^{-kt}}{2\mu_1}\sum_{i=1}^{N-1} s_i\left(c_i-\overline{c}\right)^2 + \xi_{10}e^{-kt} \\ &\le -\frac{\gamma_2}{\lambda_{\max}(P)} V + 2\overline{cu}\sum_{i=1}^{N} s_i a_{iN}\left\|Kq_i\right\| + \xi_{10}e^{-kt}\end{aligned} \tag{46}$$

Step 3: For the time interval $t\in\left[T_i+\tau_i, T_{i+1}\right)$, the following inequality holds

$$V\left(T_{i+1}\right) \le e^{-\gamma_2\left(T_{i+1}-T_i-\tau_i\right)/\lambda_{\max}(P)} V\left(T_i+\tau_i\right) + \int_{T_i+\tau_i}^{T_{i+1}} e^{-\gamma_2\left(T_{i+1}-s\right)/\lambda_{\max}(P)}\left(2\overline{cu}\sum_{i=1}^{N-1} s_i a_{iN}\left\|Kq_i(s)\right\| + \xi_{10}e^{-ks}\right)ds \tag{47}$$

For the time interval $t\in\left[T_{i+1}, T_{i+1}+\tau_{i+1}\right)$, it yields that

$$\begin{aligned}V\left(T_{i+1}+\delta_2\right) &= e^{-\gamma_2\left(T_{i+1}+\delta_2-T_{i+1}\right)/\lambda_{\max}(P)} V\left(T_{i+1}\right) + \int_{T_{i+1}}^{T_{i+1}+\delta_2} e^{-\gamma_2\left(T_{i+1}+\delta_2-s\right)/\lambda_{\max}(P)}\left(-2\Gamma\overline{cu}\sum_{i=1}^{N-1} s_i a_{iN}\left\|Kq_i(s)\right\| + \xi_9 e^{-ks}\right)ds \\ &= e^{-\gamma_2\left(T_{i+1}+\delta_2-T_i-\tau_i\right)/\lambda_{\max}(P)} V\left(T_i+\tau_i\right) + 2\overline{cu}\int_{T_i+\tau_i}^{T_{i+1}} e^{-\gamma_2\left(T_{i+1}+\delta_2-s\right)/\lambda_{\max}(P)}\sum_{i=1}^{N-1} s_i a_{iN}\left\|Kq_i(s)\right\|ds \\ &\quad -2\Gamma\overline{cu}\int_{T_{i+1}}^{T_{i+1}+\delta_2} e^{-\gamma_2\left(T_{i+1}+\delta_2-s\right)/\lambda_{\max}(P)}\sum_{i=1}^{N-1} s_i a_{iN}\left\|Kq_i(s)\right\|ds + \int_{T_i+\tau_i}^{T_{i+1}} e^{-\gamma_2\left(T_{i+1}+\delta_2-s\right)/\lambda_{\max}(P)}\xi_{10}e^{-ks}ds \\ &\quad +\int_{T_{i+1}}^{T_{i+1}+\delta_2} e^{-\gamma_2\left(T_{i+1}+\delta_2-s\right)/\lambda_{\max}(P)}\xi_9 e^{-ks}ds \\ &\le e^{-\gamma_2\left(T_{i+1}+\delta_2-T_i-\tau_i\right)/\lambda_{\max}(P)} V\left(T_i+\tau_i\right) + \int_{T_i+\tau_i}^{T_{i+1}} e^{-\gamma_2\left(T_{i+1}+\delta_2-s\right)/\lambda_{\max}(P)}\xi_{10}e^{-ks}ds + \int_{T_{i+1}}^{T_{i+1}+\delta_2} e^{-\gamma_2\left(T_{i+1}+\delta_2-s\right)/\lambda_{\max}(P)}\xi_9 e^{-ks}ds\end{aligned} \tag{48}$$

It is easy to get that

$$\begin{aligned}V\left(T_{i+1}+\delta_2\right) &\le e^{-\gamma_2\left(T_{i+1}+\delta_2-T_i-\tau_i\right)/\lambda_{\max}(P)}\left(e^{-\gamma_2\left(T_i+\delta_2-T_{i-1}-\tau_{i-1}\right)/\lambda_{\max}(P)} V\left(T_{i-1}+\tau_{i-1}\right) + \int_{T_{i-1}+\tau_{i-1}}^{T_i} e^{-\gamma_2\left(T_i+\delta_2-s\right)/\lambda_{\max}(P)}\xi_{10}e^{-ks}ds\right. \\ &\quad \left.+\int_{T_i}^{T_i+\delta_2} e^{-\gamma_2\left(T_i+\delta_2-s\right)/\lambda_{\max}(P)}\xi_9 e^{-ks}ds\right) + \int_{T_i+\tau_i}^{T_{i+1}} e^{-\gamma_2\left(T_{i+1}+\delta_2-s\right)/\lambda_{\max}(P)}\xi_{10}e^{-ks}ds + \int_{T_{i+1}}^{T_{i+1}+\delta_2} e^{-\gamma_2\left(T_{i+1}+\delta_2-s\right)/\lambda_{\max}(P)}\xi_9 e^{-ks}ds \\ &\le e^{-\gamma_2\left(T_{i+1}+\delta_2-T_{i-1}-\tau_{i-1}\right)/\lambda_{\max}(P)} V\left(T_{i-1}+\tau_{i-1}\right) + \int_{T_{i-1}+\tau_{i-1}}^{T_i} e^{-\gamma_2\left(T_{i+1}+\delta_2-s\right)/\lambda_{\max}(P)}\xi_{10}e^{-ks}ds \\ &\quad +\int_{T_i}^{T_i+\delta_2} e^{-\gamma_2\left(T_{i+1}+\delta_2-s\right)/\lambda_{\max}(P)}\xi_9 e^{-ks}ds + \int_{T_i+\tau_i}^{T_{i+1}} e^{-\gamma_2\left(T_{i+1}+\delta_2-s\right)/\lambda_{\max}(P)}\xi_{10}e^{-ks}ds + \int_{T_{i+1}}^{T_{i+1}+\delta_2} e^{-\gamma_2\left(T_{i+1}+\delta_2-s\right)/\lambda_{\max}(P)}\xi_9 e^{-ks}ds \\ &\le \cdots \\ &\le e^{-\gamma_2\left(T_{i+1}+\delta_2-T_0-\tau_0\right)/\lambda_{\max}(P)} V\left(T_0+\tau_0\right) + \mathrm{T}\end{aligned} \tag{49}$$

It is obvious that we can obtain

$$\lim_{i\to\infty} V\left(T_{i+1}+\delta_2\right) \le \lim_{i\to\infty} e^{-\gamma_2\left(T_{i+1}+\delta_2-T_0-\tau_0\right)/\lambda_{\max}(P)} V\left(T_0+\tau_0\right) + \lim_{i\to\infty}\mathrm{T} = 0 \tag{50}$$

Thus, the consensus can be obtained.

Step 4: Next, it will be proven that Zeno behavior can be ruled out. Without loss of generality, it is assumed that Zeno behavior occurs for agent *i*, that is, $\lim_{k\to\infty} t_k^i = t_\infty^i$. It is easy to get that

$$\begin{aligned}\lim_{t\to\infty}\kappa_1 e^{-kt} &> \lim_{t\to t_\infty^i}\overline{c}\left\|Ke_i(t)\right\| = 0 \\ \lim_{t\to\infty}\kappa_2 e^{-kt} &> \lim_{t\to t_\infty^i}\overline{c}^2\left\|Ke_i(t)\right\|^2 = 0\end{aligned} \tag{51}$$

However, according to event-triggering condition (14), the following inequality holds at the triggering instant t_k^i.

$$\begin{aligned}\bar{c}\left\|Ke_i\left(t_k^i\right)\right\| &> \vartheta_1 c_i(t)\left\|Kq_i\left(t_k^i\right)\right\|^2 + \kappa_1 e^{-kt_k^i} \\ \bar{c}^2\left\|Ke_i\left(t_k^i\right)\right\|^2 &> \vartheta_2 c_i(t)\left\|Kq_i\left(t_k^i\right)\right\|^2 + \kappa_2 e^{-kt_k^i}\end{aligned} \tag{52}$$

Based on the contradiction between (51) and (52), the assumption does not hold, and Zeno behavior is strictly ruled out. This completes the proof. □

Remark 4. This section theoretically validates the effectiveness of the proposed ETC strategy in solving the leader-follower consensus-seeking problem under intermittent communication, with the verification process demonstrated in four analytical phases. The first phase rigorously examines the convergence characteristics of consensus error under normal communication conditions, while the next phase analyzes the system behavior during communication-denied periods. Building on these foundations, the third phase integrates both scenarios to demonstrate the asymptotic convergence of consensus error through rigorous mathematical derivation. Furthermore, the fourth phase eliminates the possibility of Zeno behavior through a proof by contradiction, thereby completing the theoretical validation process.

4. Numerical Simulation

In this section, the effectiveness and superiority of the proposed ETC strategy are demonstrated through simulations of multiple quadrotors tracking a leader with bounded inputs. The communication topology is shown in Figure 3. In MQSs, the follower quadrotors will form a pentagonal formation around the leader.

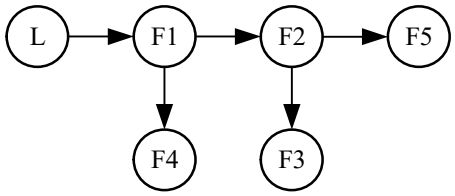

Figure 3. Communication topology of multi-quadrotor systems.

For the quadrotor with mass $m = 4\text{kg}$ and moment of inertia $J = \left[0.082, 0.082, 0.149\right]\text{kg}\cdot\text{m}^2$, the gain matrix K can be calculated as

$$K = \begin{bmatrix} & -1.41 & & -1.61 & \\ 1.41 & & 1.61 & & \\ & 1.41 & & & 4.96 \end{bmatrix} \tag{53}$$

To rigorously evaluate the proposed strategy's robustness, two groups of simulations with different initial conditions and control parameters are performed (Case 1: $\mu_1 = 1$, $\mu_2 = 0.01$, $\alpha = 1$, $k = 2.75$, $\vartheta_1 = \vartheta_2 = 1.45$, $\kappa_1 = \kappa_2 = 0.4$; Case 2: $\mu_1 = 0.1$, $\mu_2 = 0.1$, $\alpha = 1$, $k = 2.75$, $\vartheta_1 = \vartheta_2 = 0.65$, $\kappa_1 = \kappa_2 = 0.4$), the initial states of quadrotors are randomly generated around the leader. The communication intermittent intervals are constrained to [15, 20] s, [45, 55] s, [150, 170] s, and [200, 220] s.

The simulation results are shown in Figures 4–8. Figure 4 illustrates each quadrotor's trajectory within the MQSs, demonstrating that leader-follower consensus has been achieved. As depicted in Figure 4, five follower quadrotors form a stable pentagonal formation around the leader with unknown inputs within 50 s, and this formation is maintained until the end of the simulation. The position information of each agent is depicted in Figure 5, where gray areas indicate intervals of intermittent communication, while the remaining areas represent periods of normal communication. It can be observed that ETC strategy effectively addresses the leader-follower consensus-seeking problem, even when the MQSs occasionally enter communication-denial environments. The consensus error of each agent is depicted in Figure 6. This figure shows that consensus is achieved, but a steady-state error remains. This is because the controller in (7) is a proportional controller, making the steady-state error unavoidable. This issue could be addressed by designing a more robust controller. While the consensus error does not asymptotically converge to zero, the steady-state error is significantly smaller than the edge lengths of the quadrotors, ensuring practically acceptability. The maximum acceptable consensus error is typically task-dependent and constrained by mission precision requirements, safety

margins, and sensor resolution. For example, in formation control scenarios discussed in [22], consensus errors of less than 5% of the distance between agents are usually tolerable. Figure 7 depicts the triggering instants and the time intervals between consecutive triggered events. The horizontal axis represents the triggering instants, while the vertical axis represents the time intervals between consecutive triggered events. Figure 7 shows that the time intervals between triggered events are positive, thus strictly excluding Zeno behavior. Additionally, it can be observed from Figures 7 and 8 that the proposed ETC strategy reduces communication frequency while maintaining consensus. These results demonstrate the effectiveness of the proposed event-triggering condition (14) in solving the leader-follower consensus-seeking problem with reduced communication frequency compared to time-driven methods. Figure 8 illustrates the control inputs of each agent, which align with practical quadrotor actuation limits, confirming the physical realizability of the proposed control strategy.

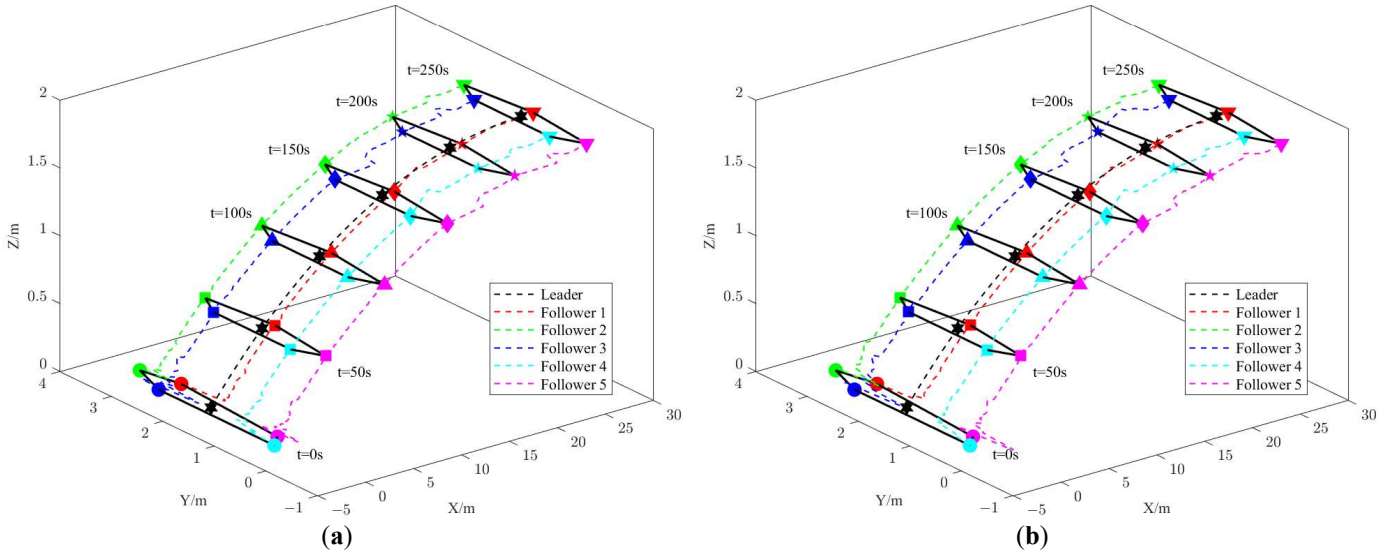

Figure 4. Trajectory of a MQSs. (**a**) Simulation results of Case 1; (**b**) Simulation results of Case 2.

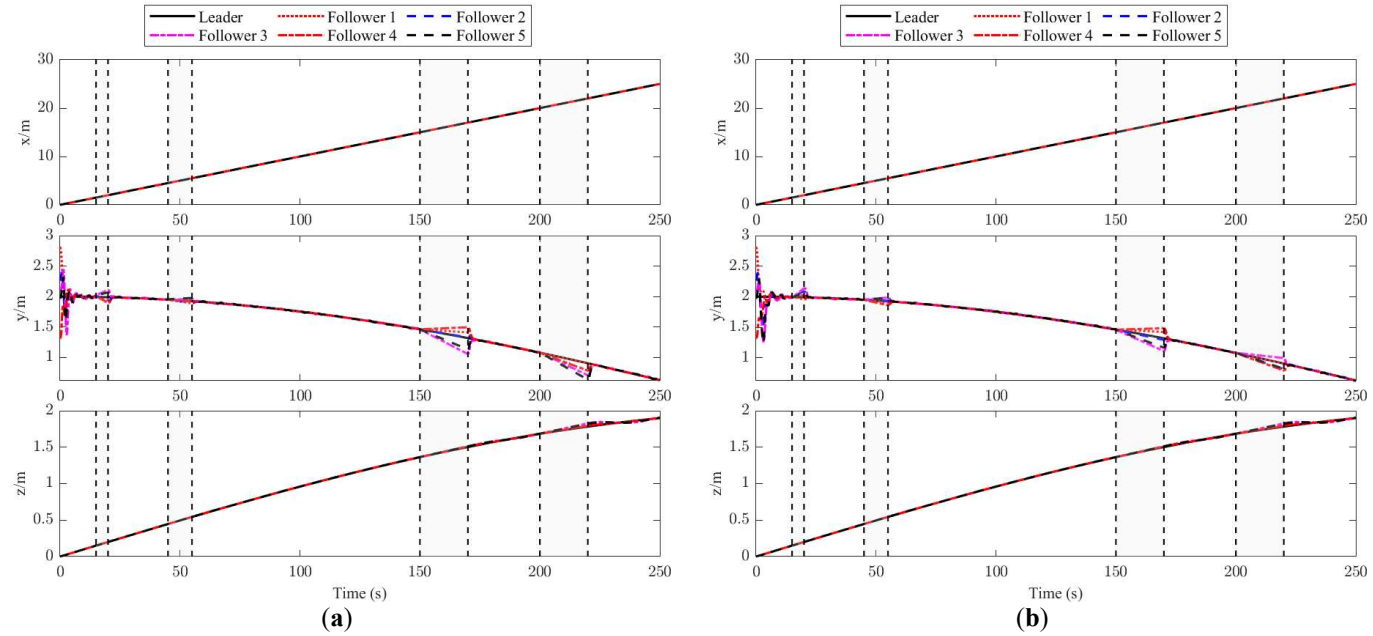

Figure 5. The states of each quadrotor. (**a**) Simulation results of Case 1; (**b**) Simulation results of Case 2.

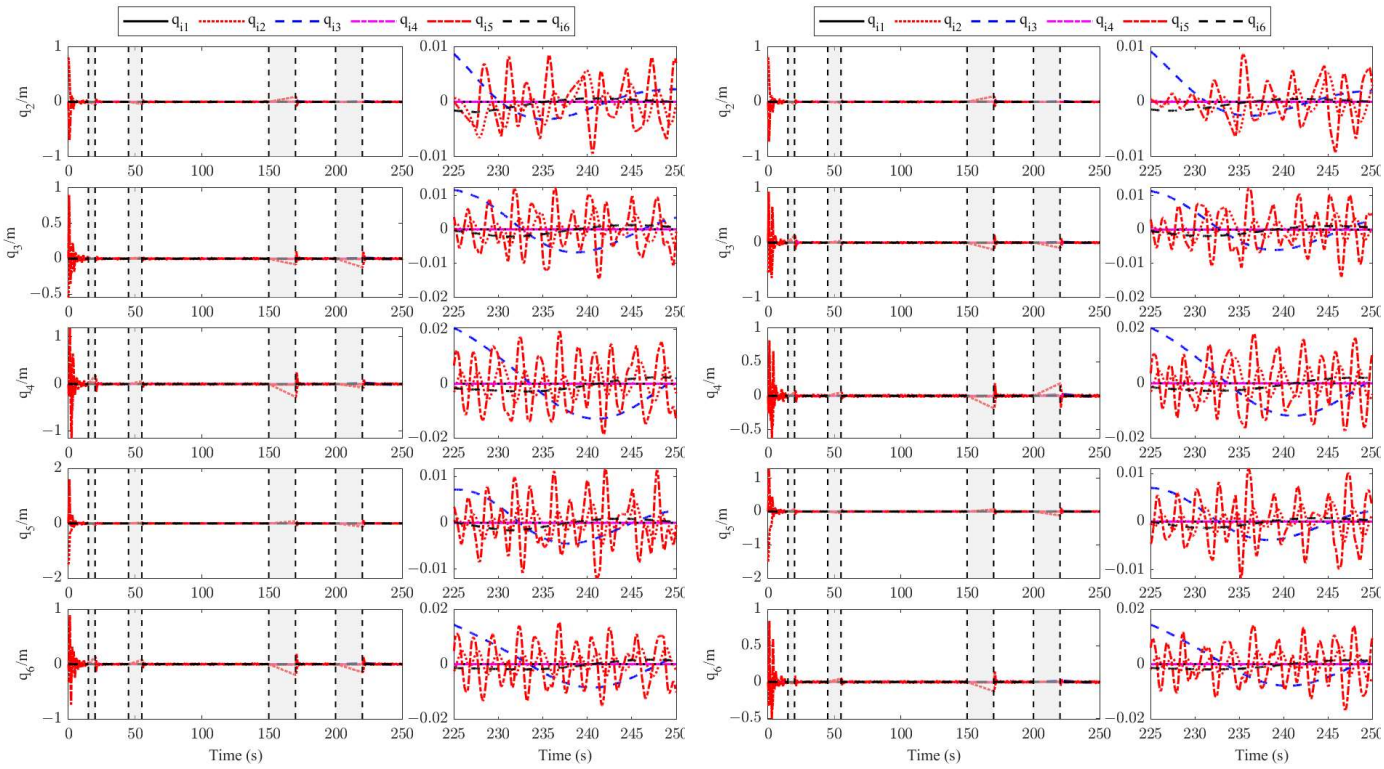

Figure 6. The consensus error of each quadrotor. (**a**) Simulation results of Case 1; (**b**) Simulation results of Case 2.

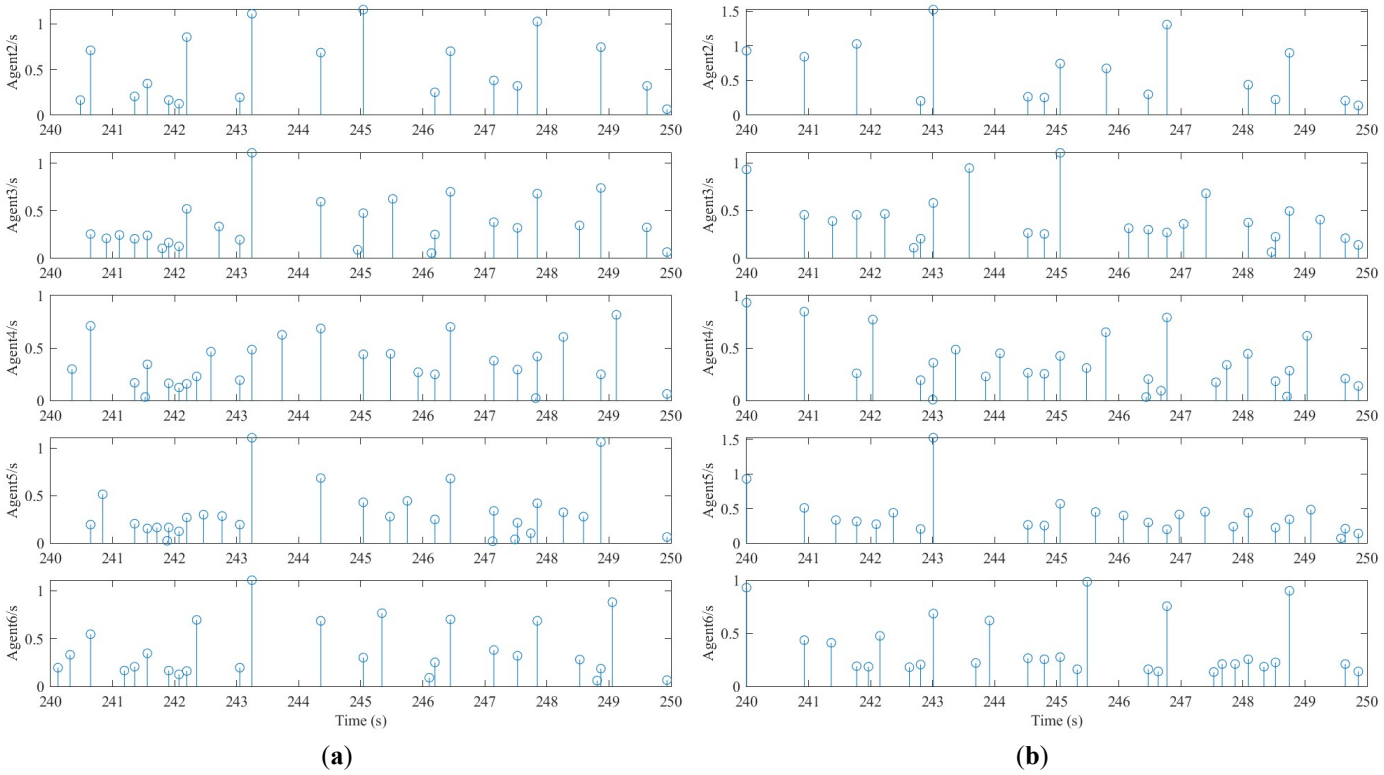

Figure 7. The triggering instants and the time intervals between triggered events. (**a**) Simulation results of Case 1; (**b**) Simulation results of Case 2.

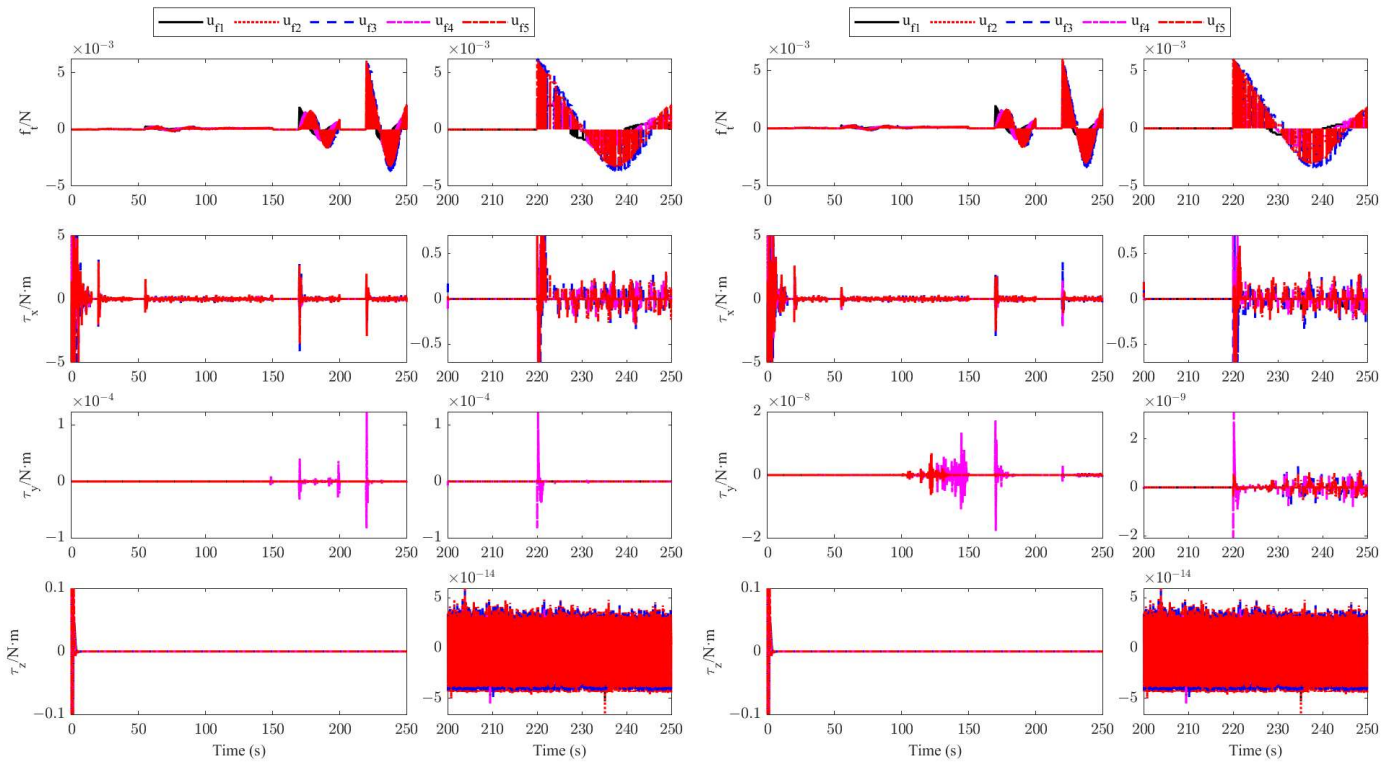

Figure 8. The control inputs of each agent. (**a**) Simulation results of Case 1; (**b**) Simulation results of Case 2.

To further validate the superiority of the proposed ETC strategy, a comparative simulation is conducted against the strategy proposed in [21]. As shown in Figure 9, the proposed strategy demonstrates a significant reduction in the number of triggered events, while achieving leader-follower consensus and maintaining a similar steady-state error. This result highlights the superior performance of the proposed strategy in reducing communication frequency among quadrotors, emphasizing its efficiency in resource-constrained MQSs.

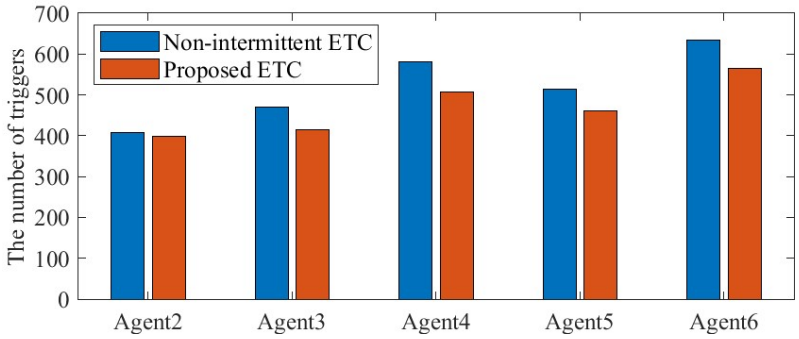

Figure 9. The number of triggered events of each agent.

5. Conclusions

In this paper, a novel adaptive ETC method has been proposed for multi-quadrotor coordination in directed graphs. With this method, the leader-follower consensus-seeking problem has been addressed. In the designed ETC method, an activation time ratio condition, a compensation in the controller, and a prediction method are developed, eliminating the dependence on the maximum time interval of intermittent communication and the reliance on continuous information. The proposed event-triggering condition can effectively reduce communication and eliminate Zeno behavior. The effectiveness of the proposed method is verified through a group of numerical simulations. Through theoretical analysis and numerical simulation, it is fully demonstrated that the proposed ETC strategy is effective in solving the leader-follower consensus-seeking problem under intermittent communications and superior in reducing communication.

Author Contributions

Conceptualization: W.Q., Y.L. (Yueyong Lv), G.M.; Formal Analysis: W.Q., Y.L. (Yueyong Lv); Investigation: W.Q., Y.L. (Yizhi Liu), Y.L. (Yueyong Lv); Methodology: W.Q., Y.L. (Yueyong Lv), G.M.; Software: W.Q.; Supervision: W.Q., G.M.; Writing—original draft: W.Q. Writing—review & editing: W.Q., Y.L. (Yizhi Liu), Y.L. (Yueyong Lv), G.M.

Ethics Statement

Not applicable.

Informed Consent Statement

Not applicable.

Data Availability Statement

This study does not involve the use of previously published or publicly accessible datasets. All data generated for this research can be accessed at the following link: https://github.com/QinWenyu/Adaptive-ETC-for-MQSs-under-Aperiodically-Intermittent-Communications.git.

Funding

This paper is funded by Shanghai Astronautic Science and Technology Foundation (SAST2023-085) and National Natural Science Foundation (U23B6001).

Declaration of Competing Interest

The authors declare that they have no known competing financial interests or personal relationships that could have appeared to influence the work reported in this paper.

References

1. Zhou M, Wang X, Wang C, Wang J. Multi-Robot Cooperative Target Search Based on Distributed Reinforcement Learning Method in 3D Dynamic Environments. *Drones Auton. Veh.* **2024**, *1*, 10012.
2. Wang W, Chen X, Jia J, Wu K, Xie M. Optimal formation tracking control based on reinforcement learning for multi-UAV systems. *Control. Eng. Pract.* **2023**, *141*, 105735.
3. Cui Y, Liang Y, Luo Q, Shu Z, Huang T. Resilient Consensus Control of Heterogeneous Multi-UAV Systems with Leader of Unknown Input Against Byzantine Attacks. *IEEE Trans. Autom. Sci. Eng.* **2024**, doi:10.1109/TASE.2024.3420697.
4. Nishira M, Nishikawa H, Kong X, Tomiyama H. An Integer Programming Approach to Multi-Trip Routing of Delivery Drones at Load-Dependent Flight Speed. *Drones Auton. Veh.* **2024**, *1*, 10008.
5. Kang Y, Luo D, Xin B, Cheng J, Yang T, Zhou S. Robust leaderless time-varying formation control for nonlinear unmanned aerial vehicle swarm system with communication delays. *IEEE Trans. Cybern.* **2022**, *53*, 5692–5705.
6. Yuhang K, Kuang Y, Cheng J, Zhang B, Yahui QI, Shaolei ZH, et al. Robust leaderless time-varying formation control for unmanned aerial vehicle swarm system with Lipschitz nonlinear dynamics and directed switching topologies. *Chin. J. Aeronaut.* **2022**, *35*, 124–136.
7. Ali ZA, Israr A, Alkhammash EH, Hadjouni M. A Leader-Follower Formation Control of Multi-UAVs via an Adaptive Hybrid Controller. *Complexity* **2021**, *2021*, 9231636.
8. Raja G, Essaky S, Ganapathisubramaniyan A, Baskar Y. Nexus of Deep Reinforcement Learning and Leader–Follower Approach for AIoT Enabled Aerial Networks. *IEEE Trans. Ind. Inform.* **2022**, *19*, 9165–9172.
9. Dimarogonas DV, Frazzoli E, Johansson KH. Distributed event-triggered control for multi-agent systems. *IEEE Trans. Autom. Control.* **2011**, *57*, 1291–1297.
10. Girard A. Dynamic triggering mechanisms for event-triggered control. *IEEE Trans. Autom. Control.* **2014**, *60*, 1992–1997.
11. Yi X, Liu K, Dimarogonas DV, Johansson KH. Dynamic event-triggered and self-triggered control for multi-agent systems. *IEEE Trans. Autom. Control.* **2018**, *64*, 3300–3307.
12. Hu W, Yang C, Huang T, Gui W. A distributed dynamic event-triggered control approach to consensus of linear multiagent systems with directed networks. *IEEE Trans. Cybern.* **2018**, *50*, 869–874.
13. Li X, Tang Y, Karimi HR. Consensus of multi-agent systems via fully distributed event-triggered control. *Automatica* **2020**, *116*, 108898.

14. Xu Y, Sun J, Wu ZG, Wang G. Fully distributed adaptive event-triggered control of networked systems with actuator bias faults. *IEEE Trans. Cybern.* **2021**, *52*, 10773–10784.
15. Wang H, Shan J. Fully distributed event-triggered formation control for multiple quadrotors. *IEEE Trans. Ind. Electron.* **2023**, *70*, 12566–12575.
16. Li Z, Su H. Distributed Attitude Tracking of Multiple Rigid Body Systems Under an Uncertain Leader and Communication Link Faults. *IEEE Trans. Aerosp. Electron. Syst.* **2024**, doi:10.1109/TASE.2024.3420697.
17. Guo Y, Duan M, Wang P. Input-to-state stabilization of semilinear systems via aperiodically intermittent event-triggered control. *IEEE Trans. Control. Netw. Syst.* **2022**, *9*, 731–741.
18. Zhang Z, Xue L, Wu Y, Liu J, Sun C. Aperiodically intermittent event-triggered control for practical fixed-time consensus under denial-of-service attack. *Nonlinear Dyn.* **2024**, *112*, 21117–21134.
19. Yin T, Gu Z, Park J H. Event-based intermittent formation control of multi-UAV systems under deception attacks. *IEEE Trans. Neural Netw. Learn. Syst.* **2022**, *35*, 8336–8347.
20. Lei J, Meng T, Wang K, Wang W, Sun S. Composite Event-Triggered Intermittent Attitude Control of Spacecraft. *IEEE Trans. Aerosp. Electron. Syst.* **2023**, *60*, 1612–1627.
21. Li X, Sun Z, Tang Y, Karimi HR. Adaptive event-triggered consensus of multiagent systems on directed graphs. *IEEE Trans. Autom. Control.* **2020**, *66*, 1670–1685.
22. Wu Y, Liang T. Improved consensus-based algorithm for unmanned aerial vehicle formation control. Acta *Aeronaut. Et Astronaut. Sin.* **2020**, *41*, 172–190.